V-band Transmission and Reflection Grid Amplifier Packaged in Waveguide

Chun-Tung Cheung[1], Roger Tsai[2], Reynold Kagiwada[2], David B. Rutledge[1]
[1] California Institute of Technology, Pasadena, California.
[2] TRW, Inc., Redondo Beach, California.

Abstract— **We designed and demonstrated two monolithic grid amplifiers in waveguide in V-band. We measured a 2dB small-signal system gain for both transmission and reflection amplifiers. This is the first monolithic grid amplifier packaged and measured in waveguide at V-band.**

I. Introduction

A single-chip quasi-optical amplifiers producing 5W of output power at Ka-band has been demonstrated [1]. This grid amplifier operates in transmission mode (Fig. 1a). In addition, a metal over-moded waveguide fed grid amplifier has been shown to have similar performance as a free-space gaussian fed grid amplifier [2]. Recently, Guyette *et al.* [3] demonstrated a reflection grid amplifier at X-band with 15dB gain (Fig. 1b). In a transmission amplifier, the polarizers isolate the input and output polarizations and provide tuning. The active grid provides gain and polarization rotation. In a reflection amplifier, the back short provides tuning and a cross-polarized horn or an ortho-mode transducer is used to separate the polarizations.

The reflection amplifier approach is excellant for thermal management by allowing the heat sink to be mounted on one side of the grid array. It also reduces physical size by folding the two polarizations into the same transmission path. However, it is difficult to tune the input and output independently. On the other hand, a transmission grid amplifier allows the input and output matching to be tuned independently and does not require the radiation impedance of the drain and gate to be matched. In this work, we designed and packaged a V-band single-stage grid amplifier with both the transmission and reflection approaches to study the advantages and limitations.

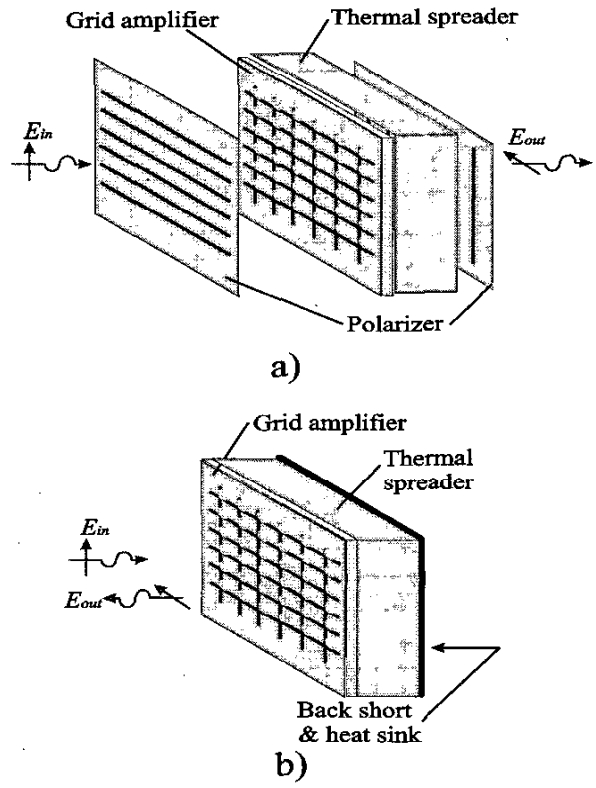

Fig. 1. Layout of a) transmission amplifier and b) reflection amplifier. The active grid provides gain and polarization rotation. In a), the polarizers isolate the input and output and provide tuning. In b), A back short is behind the thermal spreader. An ortho-mode transducer is needed to separate the polarizations.

II. Design of V-band Grid Amplifier

The V-band amplifier is a single-stage 100-cell 60-GHz grid fabricated using the TRW 0.15 μm InP power HEMT process [4]. Typical peak transconductance, maximum channel current, and off-state drain-source breakdown voltage are 750 mS/mm, 650 mA/mm, and 7 V. TRW's baseline 75-μm thick InP MMIC process was modified to achieve 125-μm final thickness for this work. Each cell contains a pair of transistors driven differentially. The design of this amplifier follows Preventza *et al.* [5]. Fig. 2a shows the half unit-cell circuit drawing. An 800-Ω resistor R_g in parallel with a 70-pF capacitor C_g at gate provides stabilization of the transistor. The gate is biased by a resistor to source because of the gate leakage current. The photograph of a section of the fabricated 5-mm square chip is shown in Fig. 2b. The height and width of a cell is 400 μm and the gate width of each transistor is 200 μm.

Fig. 3 shows a thermal image of the chip at a drain bias of 0.7V and 3.3A. A Heat sink and cooling fan were used to remove heat from the chip. The temperature distribution across the grid aperture is smooth and it indicates that the chip is biased uniformly and the thermal glue attached to InP substrate without problem. The thermal resistance is found to be 3°C/W between the grid surface and the brass mounting unit.

0-7803-7695-1/03/$17.00 © 2003 IEEE

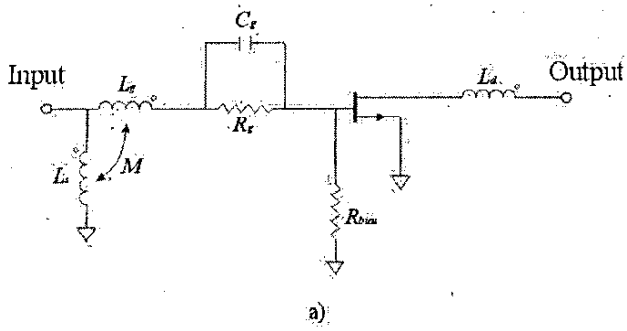

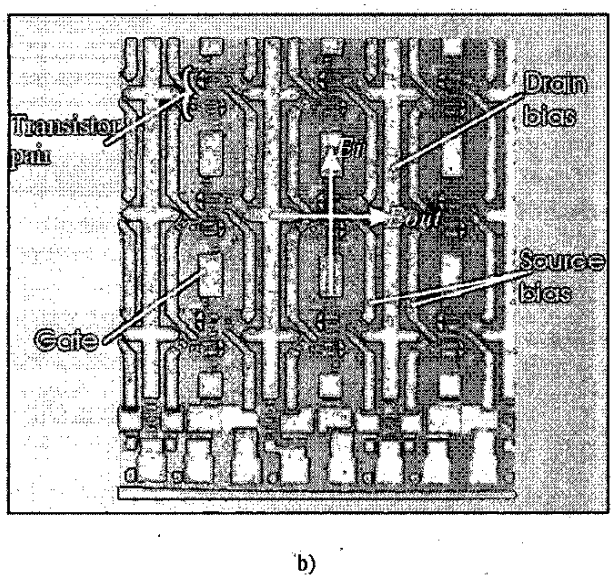

Fig. 2. a) The circuit diagram of a half unit-cell and b) a photograph of a section of the fabricated V-band single-stage grid amplifier on InP substrate with the TRW 0.15μm HEMT process. The design of the circuit follows [5]. E_i and E_{out} indicates the input and output polarizations of the field. The unit-cell width and height is 400μm.

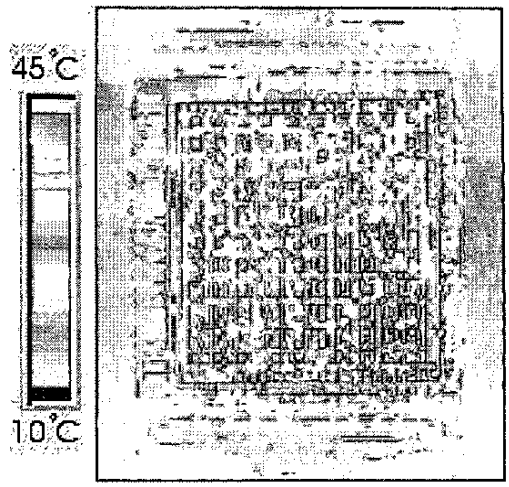

Fig. 3. A thermal image taken at drain bias of 0.7V and 3.3A. The temperature distribution is smooth and indicates the uniformity of DC-bias and thermal glue. The peak temperature is 35°C.

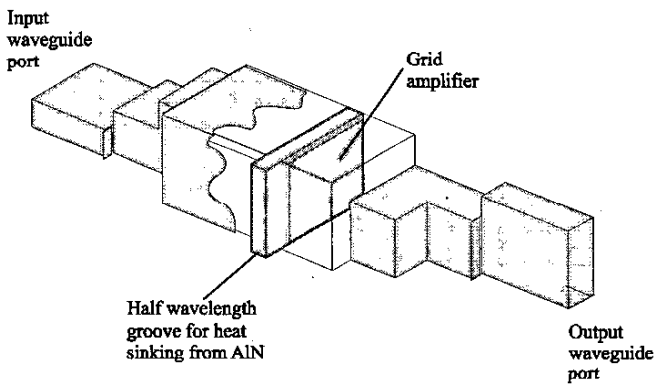

Fig. 4. A drawing of the quartered-view waveguide packaged grid amplifier. The input and output are cross-polarized. The simulation includes a half-wavelength deep groove that is for sinking heat from the AlN thermal spreader into brass unit.

III. Transmission Amplifier

A drawing of the packaged waveguide grid amplifier is shown in Fig. 4. The waveguide mode-converter is simulated with the Ansoft High Frequency Structure Simulator (HFSS). The goal is to achieve high field-uniformity over the aperture of the grid. Choke slots and DC-bias-line filters are included in our simulation. The final design has a length from input to output standard waveguide of 2cm.

The transmission grid amplifier brass units and duroid DC-bias board are shown in Fig. 5. The AlN thermal spreader was set in a half-wavelength deep groove to provide a large area for transferring heat. The bias lines were wire bonded to the grid and bypass capacitors were used to reduce RFI. Duroid polarizers were placed in over-moded waveguide sections. We use the simulations as a guide to where to put the polarizer sections. The grid was biased at 1.2V with a drain current of 6.7A. We wrote a finite-difference time-domain (FDTD) program with amplifier model to simulate the scattering parameters, and these are included. Fig. 6 shows the measured and simulated scattering parameters of the amplifier. The measured maximum small signal gain for the transmission grid amplifier is 2.1dB at 58.5GHz. The positive gain bandwidth is 2%. The simulation results have a frequency offset of 0.5GHz and it may be the discreetization error of the mesh of the mode converter.

IV. Reflection Amplifier

In order to feed a reflection grid amplifier, we need a mode-converter that separates the two polarizations into two standard waveguide ports, as proposed by DeLisio *et al.* [6]. Furthermore, the converter should suppress the higher order modes and give high return loss and low cross-coupling between polarizations. Fig. 7a shows

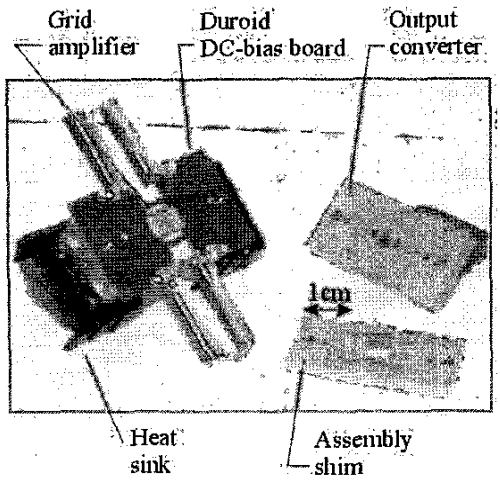

Fig. 5. The fabricated transmission grid amplifier. Heat sink is installed at the back to remove heat.

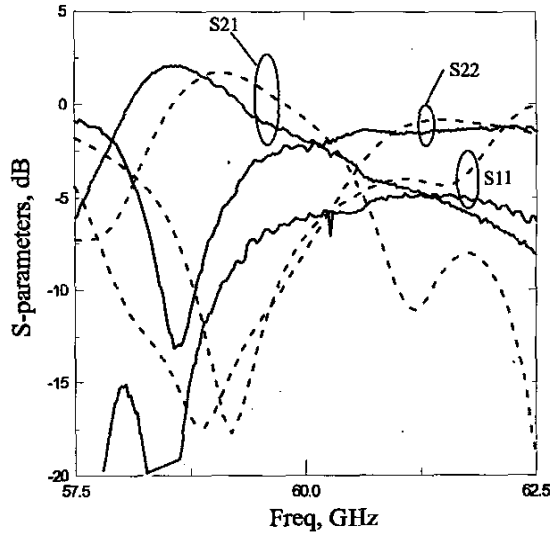

Fig. 6. The measured (solid line) and simulated (dash line) transmission grid amplifier scattering parameters. The maximum small signal gain is 2dB at 58.5GHz. The corresponding input and output return loss are 13dB and 17dB respectively. The simulation predicts the bandwidth and gain of the transmission amplifier with an offset in frequency of 0.5GHz.

a drawing of a mode-converter that excites only the TE_{10} and TE_{01} mode and couples to x and y-polarized standard waveguide. Waveguide sections are used because of the ease to be parameterized for optimization. The dimensions of the intermediate waveguide section are chosen so that TE_{10} and TE_{01} modes combines efficiently before expanding into the over-moded waveguide section. This simplifies the design by restricting the optimizer from exciting higher order modes and compensate it with successive waveguide steps. The tuner provides a symmetric cut-off waveguide for E_x and a matching for E_y. However, the tuner also limits the -10dB matching bandwidth of E_y to about 7%. On the other hand, due to the similarity to a transmission mode-converter, E_x can obtain a bandwdith of more than 10%.

The bias striplines are designed as quarter-wavelength resonator band-stop filter suppressing leakage by 30dB between 52 and 65 GHz. The HFSS simulation includes the effect of the filter. In addition, we choose the thickness of the AlN thermal spreader to help flatten the field distribution, taking the different propagation constants of the modes into account. Furthermore, the thermal spreader provides an impedance transformation that can be understood as a simple resonator circuit as shown in Fig. 7b. The typical output impedance of the chip looks like a series connected RL circuit. The back short tunes to resonate with the inductor of the chip at the design frequency. Calculation shows that the impedance at resonance is equal to

$$Z_L = R_L = R_{chip} + \frac{\omega^2 L^2}{R_{chip}} \qquad (1)$$

which transforms the load to a larger value. This avoids the subsequent matching circuit to couple energy into losses along the over-moded waveguide and DC–bias lines. In order to take the full advantage of this method, the drain and gate conjugate matching impedance have to be similar in both real and imaginary parts and impose additional constrains to the unit-cell level design. The designed mode-converter has a length of 1cm.

The mode-converter was fabricated in brass as shown in Fig. 8. The calculated AlN thickness to give ideal impedance transformation is 635 μm. Since we only excited fundamental mode for both polarizations, the distance between mode-converter and grid amplifier was predetermined and no waveguide shims was used. This also minimizes the possibility of machining misalignment and energy leakage. The grid was biased at 1.2V with a drain current of 9A. The measured and simulation results are shown in Fig. 9 The measured maximum small signal gain is 2.5dB at 58GHz. The positive gain bandwidth is 1%.

V. Conclusion

A transmission grid amplifier and a reflection grid amplifier packaged in waveguide have been demonstrated with 2dB small signal gain. The positive-gain bandwidth for the reflection amplifier is half that of the transmission amplifier (1% versus 2%). This is likely related to the difficulty in simultaneously tuning input and output in a reflection amplifier. The small measured system gain suggests a necessity of an on-chip two-stage grid amplifier design for this frequency range.

Acknowledgments The authors appreciate the support from the Army Research Office through the Caltech Quasi-Optic Power Combining MURI program.

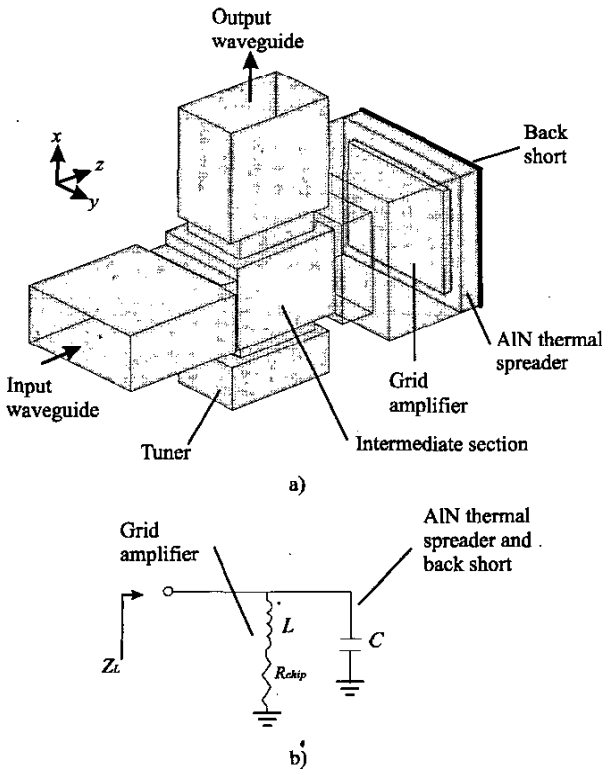

Fig. 7. a) A layout of the mode-converter for reflection grid amplifier. b) the equivalent circuit of impedance transformation. The intermediate section combines the two polarizations before expanding into over-moded section. The AlN thermal spreader and back short transform the grid amplifier impedance by resonating with the inductive component of the chip.

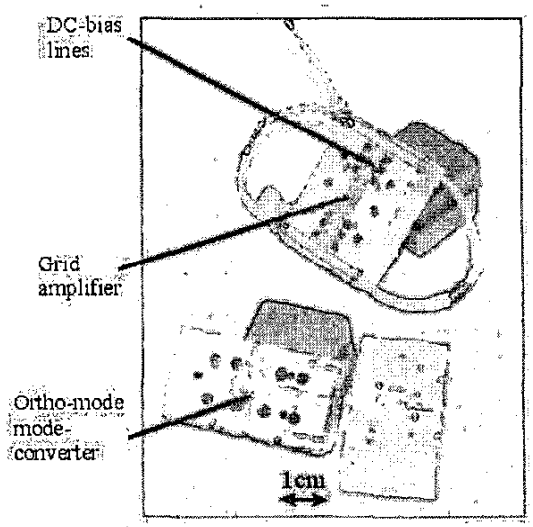

Fig. 8. The fabricated reflection grid amplifier with ortho-mode mode-converter and DC-bias lines.

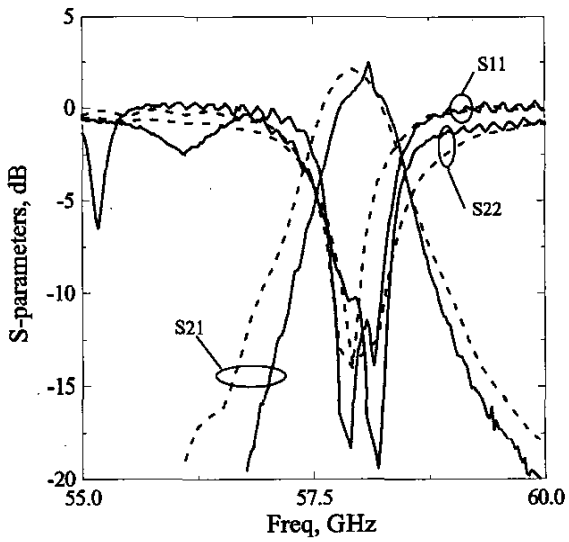

Fig. 9. The measured (solid line) and simulated (dash line) reflection grid amplifier scattering parameters. The maximum small signal gain is 2.5dB at 58GHz. The corresponding input and output return loss are 13dB and 17dB respectively. The bandwidth of the reflection amplifier is small because tuning slugs were used in both input and output following after the mode-converter.

REFERENCES

[1] B. Deckman, D. S. Deakin, Jr., E. Sovero, D. Rutledge, "A 5-Watt, 37-GHz Monolithic Grid Amplifier," 2000 Int. Microwave Symp. Dig., pp. 805-808.

[2] C. T. Cheung, J. B. Hacker, G. Nagy, D. B. Rutledge, "A Waveguide Mode-Converter Feed for a 5-W, 34-GHz Grid Amplifier," 2002 Int. Microwave Symp. Dig., pp. 1523-1526.

[3] A. Guyette, R. Swisher, F. Lecuyer, A. Al-Zayed, A. Kom, S.-T. Lei, M. Oliveira, P. Li, M. DeLisio, K. Sato, A. Oki, A. Gutierrez-Aitken, R. Kagiwada, J. Cowles, "A 16-Element Reflection Grid Amplifier with Improved Heat Sinking," 2001 Int. Microwave Symp. Dig., pp. 1839-1842.

[4] Y. C. Chen, D. L. Ingram, R. Lai, M. Barsky, R. Grundbacher, T. Block, H. C. Yen, and D. C. Streit, "A 95-GHz InP HEMT MMIC Amplifier with 427-mW Power Output," *IEEE Microwave & Guided Wave Lett.*, Nov. 1998, pp. 399-401.

[5] P. Preventza, B. Dickman, E. Sovero, M. P. DeLisio, J. J. Rosenberg, D. B. Rutledge, " Modeling of Quasi-Optical Arrays," 1999 Int. Microwave Symp. Dig., pp. 563-566.

[6] M. DeLisio, B. Deckman, J. Rosenberg, "Reflection Mode, Quasi-optical Grid Array Waveguiding System," patent pending (assignee Wavestream Wireless Technologies)